Journal of Zhejiang University-SCIENCE B (Biomedicine & Biotechnology)
ISSN 1673-1581 (Print); ISSN 1862-1783 (Online)
www.jzus.zju.edu.cn; www.springerlink.com
E-mail: jzus@zju.edu.cn

IGF-1R/β-catenin signaling axis is involved in type 2 diabetic osteoporosis*

Zhi-da ZHANG[§1], Hui REN[§2], Wei-xi WANG[1], Geng-yang SHEN[2], Jin-jing HUANG[1], Mei-qi ZHAN[1], Jing-jing TANG[2], Xiang YU[1], Yu-zhuo ZHANG[3], De LIANG[2], Zhi-dong YANG[2], Xiao-bing JIANG[†‡2,4]

[1]*The First Clinical School, Guangzhou University of Chinese Medicine, Guangzhou 510405, China*

[2]*Department of Spinal Surgery, the First Affiliated Hospital of Guangzhou University of Chinese Medicine, Guangzhou 510405, China*

[3]*School of Basic Medicine, Guangzhou University of Chinese Medicine, Guangzhou 510006, China*

[4]*Lingnan Medical Research Center of Guangzhou University of Chinese Medicine, Guangzhou 510405, China*

[†]E-mail: spinedrjxb@sina.com

Received Dec. 31, 2018; Revision accepted May 4, 2019; Crosschecked Aug. 8, 2019

Abstract: Insulin-like growth factor-1 receptor (IGF-1R) is involved in both glucose and bone metabolism. IGF-1R signaling regulates the canonical Wnt/β-catenin signaling pathway. In this study, we investigated whether the IGF-1R/β-catenin signaling axis plays a role in the pathogenesis of diabetic osteoporosis (DOP). Serum from patients with or without DOP was collected to measure the IGF-1R level using enzyme-linked immunosorbent assay (ELISA). Rats were given streptozotocin following a four-week high-fat diet induction (DOP group), or received vehicle after the same period of a normal diet (control group). Dual energy X-ray absorption, a biomechanics test, and hematoxylin-eosin (HE) staining were performed to evaluate bone mass, bone strength, and histomorphology, respectively, in vertebrae. Quantitative real-time polymerase chain reaction (qRT-PCR) and western blotting were performed to measure the total and phosphorylation levels of IGF-1R, glycogen synthase kinase-3β (GSK-3β), and β-catenin. The serum IGF-1R level was much higher in patients with DOP than in controls. DOP rats exhibited strikingly reduced bone mass and attenuated compression strength of the vertebrae compared with the control group. HE staining showed that the histomorphology of DOP vertebrae was seriously impaired, which manifested as decreased and thinned trabeculae and increased lipid droplets within trabeculae. PCR analysis demonstrated that IGF-1R mRNA expression was significantly up-regulated, and western blotting detection showed that phosphorylation levels of IGF-1R, GSK-3β, and β-catenin were enhanced in DOP rat vertebrae. Our results suggest that the IGF-1R/β-catenin signaling axis plays a role in the pathogenesis of DOP. This may contribute to development of the underlying therapeutic target for DOP.

Key words: Diabetic osteoporosis; Insulin-like growth factor-1 receptor (IGF-1R); Signaling axis; Pathogenesis
https://doi.org/10.1631/jzus.B1800648 **CLC number:** R587.2

1 Introduction

Diabetes mellitus (DM) is a chronic metabolic disease characterized by an elevated level of blood glucose, which leads over time to osteoporosis and fragility fracture (Napoli et al., 2017). According to the World Health Organization (WHO) global report on diabetes (http://www.who.int/diabetes/global-report/en), there were about 422 million adults suffering from

‡ Corresponding author
§ The two authors contributed equally to this work
* Project supported by the National Natural Science Foundation of China (Nos. 81774338 and 81674000), the Natural Science Foundation of Guangdong Province (No. 2016A030313645), the Science and Technology Projects of Guangdong Province (No. 2016A020226006), and the Guangdong Province Universities and Colleges Pearl River Scholar Funded Scheme (2018), China
ORCID: Xiao-bing JIANG, https://orcid.org/0000-0002-9428-2381
© Zhejiang University and Springer-Verlag GmbH Germany, part of Springer Nature 2019

DM worldwide in 2014, with a rising prevalence (NCD Risk Factor Collaboration, 2016). Worse still, 90% of DM patients had type 2 diabetes mellitus (T2DM), among whom 20%–60% developed osteoporosis (Schwartz et al., 2002). Osteoporosis, or bone fragility induced by diabetes, increases fracture risk by 2–6-fold (Janghorbani et al., 2006; Looker et al., 2016). Thus, an increased prevalence of diabetic osteoporosis (DOP) due to the huge and growing number of diabetics is causing excessive health-care costs worldwide. This highlights the necessity for better prevention and treatment of DOP.

Insulin-like growth factor-1 receptor (IGF-1R) is found on the surface of many kinds of cells, including hepatocytes, myocytes, and osteocytes (Cheng et al., 2016). Recent studies suggest that IGF-1R is involved in both glucose and bone metabolism (Pelosi et al., 2017; Solomon-Zemler et al., 2017). On the one hand, IGF-1R participates in modulation of glucose metabolism. IGF-1R and insulin receptor (IR) tend to form a hybrid receptor due to their high homology (de Meyts and Whittaker, 2002). These heterodimers bind to IGF-1, but not insulin because of their differential affinity (Slaaby et al., 2006). Down-regulation of IGF-1R promotes the assembly of insulin holoreceptor and increases its fraction, leading to enhanced insulin-mediated glucose uptake (Engberding et al., 2009). On the other hand, IGF-1R plays important roles in bone metabolism. Disruption of IGF-1R in osteoblasts enhances its sensitivity to insulin, which exerts a direct anabolic effect on osteoblasts (Fulzele et al., 2007), further increasing the bone density and strength (Thrailkill et al., 2005). Thus, IGF-1R may be a critical factor in the onset of DOP, in which the pathophysiology involves disturbance of both glucose and bone metabolism. However, the precise role of IGF-1R in DOP remains unclear.

Wnt/β-catenin signaling is a pivotal regulator of bone formation (Krishnan et al., 2006). The central component in this signaling pathway, β-catenin, promotes early osteoblastic proliferation and differentiation (Agholme and Aspenberg, 2011). Aberrant Wnt signaling appears to be a key player in the onset of diabetes (Cheng et al., 2015). Indeed, evidence has verified sophisticated cross-talk between bone and glucose metabolism (Daniele et al., 2015), and cross-talk between Wnt/β-catenin and IGF-1R signaling in different types of cell and biological processes (Palsgaard et al., 2012; Rota and Wood, 2015). Further, results from previous studies have demonstrated that attenuation of IGF-1R signaling enhances Wnt/β-catenin signaling in mammary epithelia (Rota et al., 2014). Therefore, we hypothesized that IGF-1R regulation of β-catenin signaling (i.e. the IGF-1R/β-catenin signaling axis) may be involved in the pathogenesis of DOP. We investigated the expression of IGF-1R, β-catenin and its upstream element glycogen synthase kinase-3β (GSK-3β) in bone tissue of DOP rats.

2 Materials and methods

2.1 Human serum collection

2.1.1 Subjects and basal clinical data

Forty inpatients with DOP (n=20) or without diabetes or osteoporosis (control, n=20) of the First Affiliated Hospital of Guangzhou University of Chinese Medicine were enrolled in this study from August 1, 2016 to August 20, 2017. We reviewed the participants' medical records for other information including age, bone mass (including bone mineral density (BMD), bone mineral content (BMC), bone area (AREA), and T score), serum marker levels of bone turnover (including the β isomer of the C-terminal telopeptide of type I collagen (β-CTX), procollagen I N-terminal propeptide (PINP), N-terminal mid-fragment of osteocalcin (N-MID), and 25-hydroxy vitamin D (25-OH VitD)), alkaline phosphatase (ALP) activity, and mineral ions (including calcium, magnesium, and phosphorus).

2.1.2 Diagnostic criteria

Diagnosis of DM was by reference to the Standards of Medical Care in Diabetes issued by the American Diabetes Association (2016); diagnosis of osteoporosis was by reference to the Clinician's Guide to Prevention and Treatment of Osteoporosis issued by the USA National Osteoporosis Foundation in 2014 (Cosman et al., 2014). Diabetic patients with osteoporosis diagnosed before diabetes and without other factors that affected skeletal metabolism, were recognized as having DOP.

2.1.3 Inclusion criteria

Patients with both definite DM and later diagnosed osteoporosis were included in the DOP group,

and those without DM or osteoporosis were included in the control group.

2.1.4 Exclusion criteria

Patients with disorders that affect bone metabolism including, but not limited to, endocrine diseases like Cushing's disease, severe cardiovascular and cerebrovascular disease, chronic obstructive pulmonary disease, autoimmune disease, neoplastic disease, and nephropathy, were excluded. Also excluded were those with long-term exposure to some medicines such as glucocorticoids, anticoagulants, proton pump inhibitors, thiazolidinediones, aromatase inhibitors, high-ceiling diuretics, antiepileptic drugs, and gonadotrophin releasing hormone analogues, which probably contribute to bone loss.

2.2 Serum sample analysis

Serum IGF-1R was measured using an enzyme-linked immunosorbent assay (ELISA) kit (#E-EL-H0425c; Elabscience Biotechnology Co., Ltd., Wuhan, China) according to the kit instructions.

2.3 Animal grouping and study design

Eighteen 14-week-old female Sprague-Dawley rats with a body weight of (260±30) g were purchased from Guangzhou University of Chinese Medicine (SCXK[Yue]2013-0034) and were kept in the First Affiliated Hospital of Guangzhou University of Chinese Medicine [SYXK[Yue]2013-0092], which provided a controlled room temperature of (23±2) °C, (50±10)% humidity, and a 12-h dark/light cycle.

Following a one-week acclimation period, rats were randomly divided into two groups: a DOP group (n=12) which received a single intraperitoneal injection of streptozotocin (STZ; #WXBC3150V; Sigma, USA) at a dose of 35 mg/kg after a four-week high-fat/sugar diet (HFD; regular diet plus 20% sugar, 10% lard, 1.0% chocolate, and 2.0% cholesterol) to induce T2DM, and a control group (CON group, n=6) which received 0.1 mol/L sodium citrate buffer vehicle (pH 4.2) after being given a four-week usual lab feed and water. This method (i.e. HFD plus STZ at a dose of 35 mg/kg) was based on our pilot study and previous literature (Srinivasan et al., 2005; Yan et al., 2018). The fasting blood glucose (FBG) of the rats was tested 3 and 4 d after STZ injection, using a Roche glucometer. Rats with FBG reaching or exceeding 11.1 mmol/L in two consecutive tests were included in the DOP group. The injection day was designated as week 0 (W0). At W14, the rats were anesthetized with 3% (0.03 g/mL) pentobarbital sodium solution and sacrificed.

2.4 Dual-energy X-ray absorptiometry measurement

Lumbar vertebra 1–3 (L1–3) samples were scanned by dual-energy X-ray absorptiometry (DXA) with a small-animal high-resolution collimator (Discovery A; Hologic, MA, USA) for measuring BMD (g/cm^2), BMC (g), and bone area (AREA, cm^2). The entire L1–3 region was marked as the region of interest (ROI). Analysis was performed using the small animal mode of the software supplied with the collimator (v.13.2:3; Hologic) and was calibrated before use.

2.5 Compression test

L1 samples from the two groups were isolated for compression tests carried out with a material testing machine (ElectroPuls E1000 Test System, Instron Corp., Norwood, MA, USA). To obtain a central cylinder of a height of about 5 mm with plano parallel ends, both end plates of the vertebra body and its appendix were removed carefully to avoid damage to the vertebral structure. Each vertebra was then tested longitudinally in the machine at a constant compressing speed of 2 mm/min. Compressive strength was calculated after the compression test.

2.6 Micro-computed tomography scanning and analysis

L2 samples of both groups at W14 were separated for micro-computed tomography (micro-CT) scanning (Skyscan 1172; Bruker, Belgium) and analyzed using the supplied software (CTAn-Shortcut v.1.17.7.1; Bruker, Belgium). The target vertebra was placed inside a tightly fitting rigid plastic tube to prevent movement and put on a turntable able to rotate automatically in the axial direction. The spatial resolution was set to 9 mm in all directions. After scanning, cancellous bone of the vertebra was selected as the volume of interest (VOI), which was restricted to an internal region of the vertebra where trabeculae and cortical bones were extracted by

drawing a cylindrical contour (diameter 2 mm) with the micro-CT analyzer software. To characterize the microarchitecture of cancellous bone, parameters including volume bone mineral density (vBMD, g/cm^3), relative bone volume (bone volume/total volume (BV/TV), %), relative bone surface (bone surface/bone volume (BS/BV), mm^{-1}), and trabecula thickness (Tb.Th, mm) were calculated using standard techniques. Three-dimensional images were obtained through multiplanar reformation.

2.7 Hematoxylin-eosin staining

L3 samples were decalcified using 10% (v/v) ethylenediaminetetraacetic acid (EDTA) phosphate buffer for six weeks, dehydrated by standard graded alcohol solutions, and embedded in paraffin (Leica, Germany). The samples were longitudinally sliced into 5-μm sections, stained with hematoxylin-eosin (HE) using the ST5010 Autostainer (Leica, Germany), and observed using an Olympus-BX53 light microscope (Olympus Corporation, Japan) for trabecula histomorphology.

2.8 Quantitative real-time polymerase chain reaction analysis

L4 samples without soft tissues were pulverized in liquid nitrogen to avoid messenger RNA (mRNA) degradation. Total RNA was extracted using a TaKaRa MiniBEST Universal RNA Extraction Kit (#AK1402; TaKaRa, Japan) and was reverse-transcribed into complementary DNA (cDNA) with PrimeScript RT Master Mix (Perfect Real Time; #AK4102; TaKaRa, Japan) in a volume of 20 μL. cDNA amplification was carried out with specific primers (Table 1) and normalized relative to the housekeeping gene, *β-actin*. Genes including *IGF-1R*, *GSK-3β*, and *β-catenin* were assayed. Quantification of relative expression levels of the genes was achieved using the $2^{-\Delta\Delta C_T}$ method.

2.9 Western blot detection

L5 samples were crushed in liquid nitrogen and lysed by radioimmunoprecipitation assay (RIPA) buffer (Beyotime Biotechnology, Nantong, Jiangsu, China). After centrifugation, protein levels in the supernatant were measured using the BCA Protein Assay Kit (Bioworld Technology Co., Ltd., Minnesota, USA). Each protein sample (60 μg) was loaded into 10% (0.1 g/mL) of sodium dodecylsulphate-polyacrylamide gel electrophoresis (SDS-PAGE) and transferred onto a polyvinylidene fluoride (PVDF) membrane (Millipore, Merck, KgaA, Darmstadt, Germany). Afterwards, the membrane was blocked with 5% (0.05 g/mL) bovine serum albumin (BSA) solution for 1 h and incubated with primary antibodies against IGF-1Rβ (#9750; 1:1000; CST, USA), p-IGF-1Rβ (#3021; 1:1000; CST, USA), β-catenin (#8480; 1:1000; CST, USA), p-β-catenin (#9561; 1:1000; CST, USA), GSK-3β (#9315; 1:1000; CST, USA), p-GSK-3β (#5558; 1:1000; CST, USA), and β-actin (#ab6276; 1:20000; Cambridge, UK) overnight at 4 °C, followed by the corresponding secondary antibody at room temperature for 1 h, and washed with TBST (Tris-HCl 10 mmol/L, NaCl 150 mmol/L, Tween-20 0.05% (v/v); pH=7.5) three times. Protein expression signals were visualized with enhanced chemiluminescence (ECL) luminous liquid (Bio-Rad, California, USA) and the images were captured using the Tanon system (Tanon 6600, Shanghai, China). The gray value of the blots was quantified using ImageJ software (National Institutes of Health, Bethesda, MD, USA).

2.10 Statistical analysis

Statistical analysis involved unpaired, two-tailed Student's *t*-tests or Welch's *t*-tests for comparison between two groups using GraphPad Prism software (Version 7.0). All data were expressed as mean±standard deviation (SD) for comparison of all parameters.

Table 1 Sequences of primers used in the qRT-PCR

Gene	Gene ID	Sequence of primer (5'→3')	Size (bp)
IGF-1R	NM_052807.2	Forward: ACAGTGAATGAGGCTGCAA Reverse: TGGCCTTGGGATACTACACC	120
GSK-3β	NM_032080.1	Forward: TCTGGCCACCATCCTTATCC Reverse: AAGCGGCGTTATTGGTCTGT	122
β-Catenin	NM_053357.2	Forward: CTGAGGACAAGCCACAGGA Reverse: CACCAATGTCCAGTCCGAGA	118
β-Actin	NM_031144.3	Forward: GATCAAGATCATTGCTCCTCCTGA Reverse: ACGCAGCTCAGTAACAGTCC	173

3 Results

3.1 Reduced bone mass with elevated levels of serum IGF-1R in patients with DOP

DOP patients had a significantly lower bone mass, including BMD, BMC, AREA, and T score, and serum level of 25-OH VitD than controls (Table 2). The serum IGF-1R level was much higher in DOP patients than in controls.

3.2 Rat DOP model established by HFD combined with STZ administration

The FBG levels were monitored at W0, Days 3 and 4 (D3&4), W4, W8, and W14. After STZ injection, six rats with FBG exceeding 11.1 mmol/L in two consecutive tests (i.e. tests at D3&4) were included in the DOP group. The FBG levels of DOP rats remained notably higher than those of CON rats after STZ injection (Fig. 1a).

To confirm the establishment of the DOP model, DXA measurements and biomechanics tests were performed. Both BMD and BMC were notably lower in the DOP group than in the CON group (Fig. 1b). The mechanical properties of the lumbar vertebrae were examined by compression test. DOP rats showed a strikingly attenuated compressive strength compared with the CON group (Fig. 1c).

HE staining showed the impaired histomorphology of the lumbar vertebrae in DOP rats. Representative pictures are presented as Fig. 1d. Obviously sparse and thin trabeculae and an irregular mesh structure of the trabecular bone were observed in DOP rats compared with CON rats under both 40× (upper images) and 100× (lower images) magnifications. Lipid droplets were more abundant within the spaces between trabeculae in DOP vertebrae than in CON vertebrae.

Further, micro-CT scans provided two-dimensional and three-dimensional images representing the microarchitecture of the L2 in both groups. Generally, three-dimensional bone microarchitecture showed obviously sparse trabeculae. Parameters relating to bone microarchitecture were quantitatively analyzed: the DOP group showed remarkably reduced BV/TV and Tb.Th, but significantly increased BS/BV, compared with the CON group (Fig. 1e).

3.3 Altered IGF-1R/β-catenin signaling in DOP bone tissue

To test our hypothesis, gene expression analysis was performed by quantitative real-time polymerase chain reaction (qRT-PCR) using vertebral tissue. IGF-1R mRNA expression was significantly up-regulated in the DOP group relative to the CON group, although GSK-3β and β-catenin showed only a trend of up-regulation (Fig. 2).

Phosphorylation levels of this signaling axis, including IGF-1R, GSK-3β, and β-catenin, were examined by western blotting. Representative panels presented and quantitative analysis showed markedly enhanced phosphorylation levels of IGF-1R, GSK-3β, and β-catenin in the DOP group relative to the CON group (Fig. 3). There were no significant differences in level of total IGF-1R, GSK-3β, or β-catenin between the two groups.

Table 2 Basal clinical data and IGF-1R level

Group	Age (year)	Gender (male/female)	BMD (g/cm^2)	BMC (g)	AREA (cm^2)
Control	66.0±9.0	0/20	1.045±0.048	67.211±3.192	64.753±1.077
DOP	69.3±5.3	0/20	0.678±0.134**	43.185±10.044**	63.307±0.693*
Group	T score	PINP (ng/mL)	β-CTX (ng/mL)	N-MID (ng/mL)	25-OH VitD (ng/mL)
Control	−0.33±0.41	54.55±20.25	0.590±0.267	20.81±8.62	26.52±4.49
DOP	−4.00±1.38**	62.78±34.29	0.578±0.285	15.55±5.29	16.61±6.90*
Group	Calcium (mmol/L)	ALP (U/L)	Phosphorus (mmol/L)	Magnesium (mmol/L)	IGF-1R (ng/mL)
Control	2.34±0.06	61.17±14.70	1.37±0.16	0.87±0.08	7.31±2.37
DOP	2.29±0.07	87.29±35.93	1.28±0.14	0.89±0.06	11.63±3.60**

All data are expressed as mean±SD (n=20), except gender. * P<0.05, ** P<0.01, vs. control. DOP: diabetic osteoporosis; BMD: bone mineral density; BMC: bone mineral content; PINP: procollagen I N-terminal propeptide; β-CTX: β isomer of the C-terminal telopeptide of type I collagen; N-MID: N-terminal mid-fragment of osteocalcin; 25-OH VitD: 25-hydroxy vitamin D; ALP: alkaline phosphatase; IGF-1R: insulin-like growth factor-1 receptor

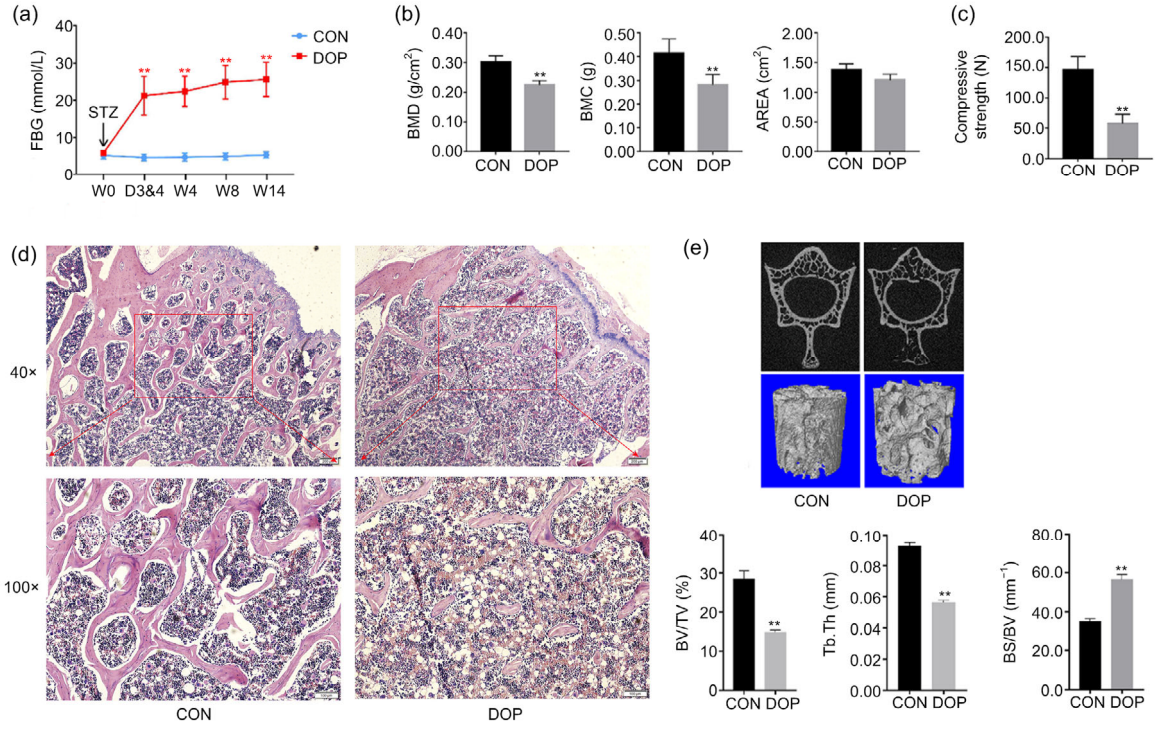

Fig. 1 Incorporating STZ and HFD induced serious diabetes and secondary bone loss

(a) Hyperglycemia was induced by STZ. (b) Massive bone loss occurred. (c) Bone fragility was increased in diabetic rats. Altered histomorphology (d) and compromised microarchitecture (e) of the lumbar vertebrae were caused by diabetes. In (d), scale bar: 200 μm (upper) and 100 μm (below). STZ: streptozotocin; HFD: high-fat/sugar diet; FBG: fasting blood glucose; BMD: bone mineral density; BMC: bone mineral content; BV/TV: relative bone volume (bone volume/total volume); Tb.Th: trabecula thickness; BS/BV: relative bone surface (bone surface/bone volume); CON: control; DOP: diabetic osteoporosis; W0, D3&4, W4, W8, W14: Week 0, Days 3 and 4, Week 4, Week 8, Week 14. All data are expressed as mean±SD (n=5). $^{**}P<0.01$, vs. CON

4 Discussion

In the present study, the serum IGF-1R of patients with DOP was shown to be notably higher than that of controls; ten rats were subjected to a single intraperitoneal injection of STZ after a four-week HFD induction, and six DOP models were successfully established after 14 weeks. This was confirmed by decreased BMD and BMC, attenuated bone strength, altered histomorphology, and compromised microarchitecture. These results coincided with those of previous studies (Li et al., 2013; Ma et al., 2017). Based on this model, we further delved into the molecular mechanism and found that the expression of IGF-1R, GSK-3β, and β-catenin mRNAs, and phosphorylation of the related proteins were significantly increased in DOP rats relative to CON rats. The alteration of the IGF-1R/β-catenin signaling pathway indicated that this signal axis could function as a pivotal player in the pathogenesis of DOP. Our results may provide evidence for a novel therapeutic target for DOP.

STZ is the chemical most often used to induce diabetes. First used in 1963, it can be used for induction of both T1DM and T2DM (Gheibi et al., 2017) through impairment of β-cells (Szkudelski, 2012). A low dose of STZ causes mild disruption of insulin secretion, which resembles the later stages of T2DM (Reed et al., 2000). Moreover, an HFD contributes to the development of obesity, insulin resistance, and hyperinsulinemia, but not frank hyperglycemia or diabetes (Flanagan et al., 2008). Thus, incorporating HFD and STZ simulates not only the phenotype, but also the pathogenesis of human T2DM. This has made it a widely recognized method for induction of T2DM in rats (Reed et al., 2000; Flanagan et al., 2008;

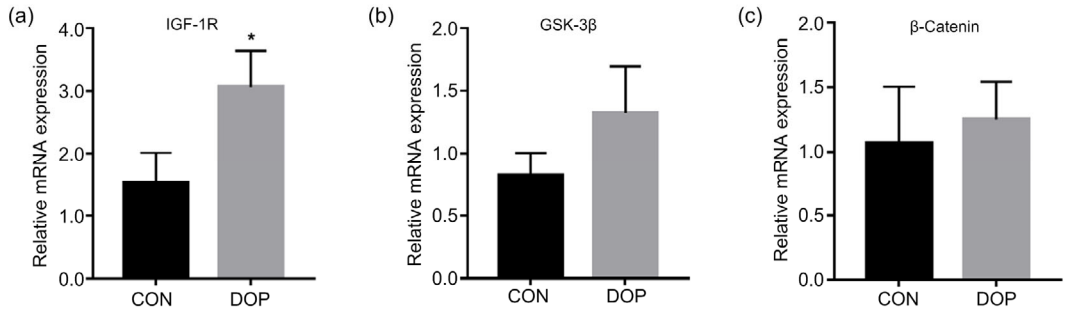

Fig. 2 Altered relative expression of IGF-1R/β-catenin signaling axis

The expression of IGF-1R (a) was significantly up-regulated, but the up-regulated expression of both GSK-3β (b) and β-catenin (c) was not significant. IGF-1R: insulin-like growth factor-1 receptor; GSK-3β: glycogen synthase kinase-3β; CON: control; DOP: diabetic osteoporosis. All data are expressed as mean±SD (n=3). * P<0.05, vs. CON

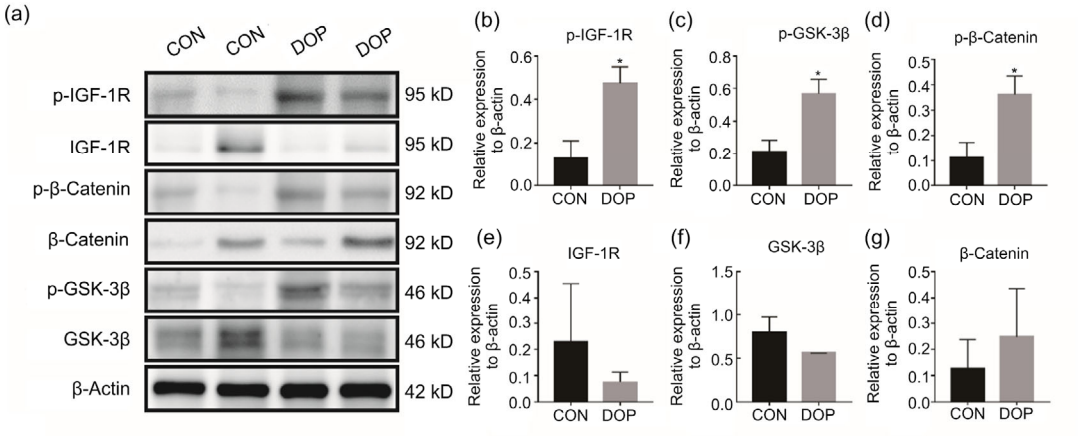

Fig. 3 Enhanced phosphorylation levels of the IGF-1R/β-catenin signaling axis

(a) The representative brands were presented, indicating the enhancement of phosphorylation levels of IGF-1R/β-catenin signaling. Quantitative analysis showed increased p-IGF-1R (b), p-GSK-3β (c), and p-β-catenin (d), but unchanged total IGF-1R (e), GSK-3β (f), and β-catenin (g). IGF-1R: insulin-like growth factor-1 receptor; GSK-3β: glycogen synthase kinase-3β; CON: control; DOP: diabetic osteoporosis. All data are expressed as mean±SD (n=3). * P<0.05, vs. CON

Liu et al., 2015; Bozic et al., 2018). By feeding an HFD for four weeks and administering STZ at a dose of 35 mg/kg, we successfully created a T2DM model in the rat. Despite setting the cutoff value of FBG at 11.1 mmol/L based on previous studies (Zhao et al., 2013; Lu et al., 2016; Jiao et al., 2017), all rats selected in the DOP groups had an FBG much higher than 11.1 mmol/L (14.2–31.1 mmol/L). Serious hyperglycemia led to remarkable osteoporosis. This differs from cases in which patients with T2DM frequently have a normal or slightly elevated BMD. However, our result was consistent with the study reported by Li et al. (2013).

It is well accepted that IGF-1 exerts anabolic actions in bone (Fulzele et al., 2007; Fowlkes et al., 2013). A decline in IGF-1 level leads to bone fragility and increased fracture risk (Sroga et al., 2015), and plays an important role in the development of DOP (Hough et al., 2016). However, the role of IGF-1R in DOP remains unclear. IGF-1R is a homodimer of two protein subunits composed of α and β chains with disulfide-linkages between these subunits and chains (de Meyts and Whittaker, 2002). It is implicated in both bone and glucose metabolism, functioning as a pivotal mediator underlying the disturbance of glucose and bone metabolism. The conformation of IGF-1R is changed by binding with the ligand IGF-1, followed by consequent full activation through autophosphorylation independent of the ligand (Kavran et al., 2014). This induces phosphorylation of multiple

substrates like insulin receptor substrate (IRS) and Shc proteins, and initiation of specific signaling cascades such as the phosphoinositide 3-kinase (PI3K)/Akt and Ras/mitogen-activated protein kinase (MAPK) pathways (Siddle, 2012; Boucher et al., 2014). IRS1 and IRS2 promote Wnt/β-catenin signaling through stabilizing Disheveled 2 (Dvl2, β-catenin upstream component) which triggers downstream signaling transduction in this cascade (Geng et al., 2014). Subsequent degradation posterior to the specific phosphorylation domain (like serine 332) (Boura-Halfon et al., 2010; Leng et al., 2010) of IRS1 reduces Dvl2 stabilization and tempers Wnt signaling transduction. In the present study, phosphorylation of IGF-1R was remarkably enhanced in DOP bone. Accordingly, hyperphosphorylation of IGF-1R may induce β-catenin phosphorylation through inhibitory phosphorylation (e.g. degradation) of IRS1.

The Wnt/β-catenin signaling pathway is indispensable for bone formation (Iyer et al., 2013). Wnt proteins trigger this signaling cascade by activating Frizzled/lipoprotein receptor-related protein-5 (LRP5) or LRP6 receptor complex to prevent β-catenin degradation, thereby increasing its cytoplasmic accumulation and nuclear translocation, promoting interaction with T-cell factor/lymphoid enhancer-binding factor (TCF/LEF) to trigger the transcription of specific genes such as *c-myc* and *cyclin D1* (Zhang et al., 2016). GSK-3β is a component of this canonical Wnt signaling pathway and phosphorylates β-catenin, thereby promoting its degradation. On the one hand, GSK-3β is regulated by IGF-1R as a downstream element of the IGF-1R/PI3K/Akt pathway (Kim et al., 2014). Our results also suggest that GSK-3β could be regulated by IGF-1R. On the other hand, activated GSK-3β contributes to IRS1 degradation (Geng et al., 2014), leading to reduced stabilization of β-catenin's upstream component Dvl2, and attenuates Wnt/β-catenin signaling. Furthermore, a previous study demonstrated that IGF-1 antagonized the Wnt/β-catenin signaling pathway by catalyzing transcription of Axin2 and stabilizing Axin1 protein (Schlupf and Steinbeisser, 2014). Both Axin2 and Axin1 are components of the β-catenin's upstream destruction complex adenomatous polyposis coli (APC)-Axin-GSK-3β compound and act as intracellular suppressors of this pathway (Ikeda et al., 1998; Schlupf and Steinbeisser, 2014). This may be another contributor to the notably increased level of p-β-catenin observed in our study, which indicates potential interplay between Axin and GSK-3β. However, whether reduced transcription of Axin2 or stabilization of Axin1 associates with GSK-3β needs to be verified by further study. Lastly, although previous studies have revealed that IGF-1 enhances β-catenin signaling (Desbois-Mouthon et al., 2001; Ma et al., 2017), the expression or action of IGF-1R was unknown without detection in these studies. Collectively, GSK-3β mediates pathways to attenuate the β-catenin signaling axis, but the molecular basis remains elusive.

Our study had some limitations. The insulin resistance index and insulin sensitivity index that are key indicators of the efficacy of diabetes model establishment, were not measured before STZ injection, leading to a relatively low rate of model establishment. Another limitation was that an inhibitor of IGF-1R/β-catenin signaling was not used in the present study. A future study should apply an inhibitor to determine whether the bone loss or microarchitecture impairment is prevented or reversed.

5 Conclusions

Taken together, our results demonstrated that the IGF-1R/β-catenin signaling axis plays a role in the pathogenesis of DOP. This may contribute to the development of the underlying therapeutic target for DOP.

Contributors

Zhi-da ZHANG, Hui REN, and Xiao-bing JIANG designed this study. Wei-xi WANG, Geng-yang SHEN, Jin-jing HUANG, Mei-qi ZHAN, and Yu-zhuo ZHANG performed these experiments. Jing-jing TANG and Xiang YU searched the relative literature and reviewed the methods for model establishment, Zhi-da ZHANG and Hui REN conducted statistical analysis. Zhi-da ZHANG prepared this manuscript. De LIANG and Zhi-dong YANG reviewed and edited manuscript. All authors have read and approved this manuscript. Therefore, all authors have full access to all the data in the study and take responsibility for the integrity and security of the data.

Acknowledgments

We thank the specific pathogen free (SPF) animal laboratory of the First Affiliated Hospital of Guangzhou University of Chinese Medicine, Guangzhou, China, for providing the experimental platform.

Compliance with ethics guidelines

Zhi-da ZHANG, Hui REN, Wei-xi WANG, Geng-yang SHEN, Jin-jing HUANG, Mei-qi ZHAN, Jing-jing TANG, Xiang YU, Yu-zhuo ZHANG, De LIANG, Zhi-dong YANG, and Xiao-bing JIANG declare that they have no conflict of interest.

All institutional and national guidelines for the care and use of laboratory animals were followed. All procedures followed were in accordance with the ethical standards of the responsible committee on human experimentation (institutional and national) and with the Helsinki Declaration of 1975, as revised in 2008 (5). Informed consent was obtained from all patients for being included in the study.

References

Agholme F, Aspenberg P, 2011. Wnt signaling and orthopedics, an overview. *Acta Orthop*, 82(2):125-130. https://doi.org/10.3109/17453674.2011.572252

American Diabetes Association, 2016. Standards of medical care in diabetes—2016 abridged for primary care providers. *Clin Diabetes*, 34(1):3-21. https://doi.org/10.2337/diaclin.34.1.3

Boucher J, Kleinridders A, Kahn CR, 2014. Insulin receptor signaling in normal and insulin-resistant states. *Cold Spring Harb Perspect Biol*, 6(1):a009191. https://doi.org/10.1101/cshperspect.a009191

Boura-Halfon S, Shuster-Meiseles T, Beck A, et al., 2010. A novel domain mediates insulin-induced proteasomal degradation of insulin receptor substrate 1 (IRS-1). *Mol Endocrinol*, 24(11):2179-2192. https://doi.org/10.1210/me.2010-0072

Bozic J, Markotic A, Cikes-Culic V, et al., 2018. Ganglioside GM3 content in skeletal muscles is increased in type 2 but decreased in type 1 diabetes rat models: implications of glycosphingolipid metabolism in pathophysiology of diabetes. *J Diabetes*, 10(2):130-139. https://doi.org/10.1111/1753-0407.12569

Cheng PW, Chen YY, Cheng WH, et al., 2015. Wnt signaling regulates blood pressure by downregulating a GSK-3β-mediated pathway to enhance insulin signaling in the central nervous system. *Diabetes*, 64(10):3413-3424. https://doi.org/10.2337/db14-1439

Cheng YY, Liu SC, Zhang X, et al., 2016. Expression profiles of *IGF-1R* gene and polymorphisms of its regulatory regions in different pig breeds. *Protein J*, 35(3):231-236. https://doi.org/10.1007/s10930-016-9666-x

Cosman F, de Beur SJ, LeBoff MS, et al., 2014. Clinician's guide to prevention and treatment of osteoporosis. *Osteoporos Int*, 25(10):2359-2381. https://doi.org/10.1007/s00198-014-2794-2

Daniele G, Winnier D, Mari A, et al., 2015. Sclerostin and insulin resistance in prediabetes: evidence of a cross talk between bone and glucose metabolism. *Diabetes Care*, 38(8):1509-1517. https://doi.org/10.2337/dc14-2989

de Meyts P, Whittaker J, 2002. Structural biology of insulin and IGF1 receptors: implications for drug design. *Nat Rev Drug Discov*, 1(10):769-783. https://doi.org/10.1038/nrd917

Desbois-Mouthon C, Cadoret A, Blivet-van Eggelpoël MJ, et al., 2001. Insulin and IGF-1 stimulate the β-catenin pathway through two signalling cascades involving GSK-3β inhibition and Ras activation. *Oncogene*, 20(2):252-259. https://doi.org/10.1038/sj.onc.1204064

Engberding N, San Martin A, Martin-Garrido A, et al., 2009. Insulin-like growth factor-1 receptor expression masks the antiinflammatory and glucose uptake capacity of insulin in vascular smooth muscle cells. *Arterioscler Thromb Vasc Biol*, 29(3):408-415. https://doi.org/10.1161/ATVBAHA.108.181727

Flanagan AM, Brown JL, Santiago CA, et al., 2008. High-fat diets promote insulin resistance through cytokine gene expression in growing female rats. *J Nutr Biochem*, 19(8):505-513. https://doi.org/10.1016/j.jnutbio.2007.06.005

Fowlkes JL, Nyman JS, Bunn RC, et al., 2013. Osteo-promoting effects of insulin-like growth factor I (IGF-I) in a mouse model of type 1 diabetes. *Bone*, 57(1):36-40. https://doi.org/10.1016/j.bone.2013.07.017

Fulzele K, DiGirolamo DJ, Liu ZY, et al., 2007. Disruption of the insulin-like growth factor type 1 receptor in osteoblasts enhances insulin signaling and action. *J Biol Chem*, 282(35):25649-25658. https://doi.org/10.1074/jbc.M700651200

Geng YT, Ju YF, Ren FL, et al., 2014. Insulin receptor substrate 1/2 (IRS1/2) regulates Wnt/β-catenin signaling through blocking autophagic degradation of Dishevelled2. *J Biol Chem*, 289(16):11230-11241. https://doi.org/10.1074/jbc.M113.544999

Gheibi S, Kashfi K, Ghasemi A, 2017. A practical guide for induction of type-2 diabetes in rat: incorporating a high-fat diet and streptozotocin. *Biomed Pharmacother*, 95:605-613. https://doi.org/10.1016/j.biopha.2017.08.098

Hough FS, Pierroz DD, Cooper C, et al., 2016. MECHANISMS IN ENDOCRINOLOGY: mechanisms and evaluation of bone fragility in type 1 diabetes mellitus. *Eur J Endocrinol*, 174(4):R127-R138. https://doi.org/10.1530/EJE-15-0820

Ikeda S, Kishida S, Yamamoto H, et al., 1998. Axin, a negative regulator of the Wnt signaling pathway, forms a complex with GSK-3β and β-catenin and promotes GSK-3β-dependent phosphorylation of β-catenin. *EMBO J*, 17(5):1371-1384. https://doi.org/10.1093/emboj/17.5.1371

Iyer S, Ambrogini E, Bartell SM, et al., 2013. FOXOs attenuate bone formation by suppressing Wnt signaling. *J Clin Invest*, 123(8):3409-3419. https://doi.org/10.1172/JCI68049

Janghorbani M, Feskanich D, Willett WC, et al., 2006. Prospective study of diabetes and risk of hip fracture: the nurses' health study. *Diabetes Care*, 29(7):1573-1578. https://doi.org/10.2337/dc06-0440

Jiao YK, Wang XQ, Jiang X, et al., 2017. Antidiabetic effects

of *Morus alba* fruit polysaccharides on high-fat diet- and streptozotocin-induced type 2 diabetes in rats. *J Ethnopharmacol*, 199:119-127. https://doi.org/10.1016/j.jep.2017.02.003

Kavran JM, McCabe JM, Byrne PO, et al., 2014. How IGF-1 activates its receptor. *eLife*, 3:e03772. https://doi.org/10.7554/eLife.03772

Kim IG, Kim SY, Choi SI, et al., 2014. Fibulin-3-mediated inhibition of epithelial-to-mesenchymal transition and self-renewal of ALDH+ lung cancer stem cells through IGF1R signaling. *Oncogene*, 33(30):3908-3917. https://doi.org/10.1038/onc.2013.373

Krishnan V, Bryant HU, MacDougald OA, 2006. Regulation of bone mass by Wnt signaling. *J Clin Invest*, 116(5): 1202-1209. https://doi.org/10.1172/JCI28551

Leng SH, Zhang WS, Zheng YB, et al., 2010. Glycogen synthase kinase 3β mediates high glucose-induced ubiquitination and proteasome degradation of insulin receptor substrate 1. *J Endocrinol*, 206(2):171-181. https://doi.org/10.1677/JOE-09-0456

Li BX, Wang Y, Liu Y, et al., 2013. Altered gene expression involved in insulin signaling pathway in type II diabetic osteoporosis rats model. *Endocrine*, 43(1):136-146. https://doi.org/10.1007/s12020-012-9757-1

Liu XJ, Xu Q, Wang XM, et al., 2015. Irbesartan ameliorates diabetic cardiomyopathy by regulating protein kinase D and ER stress activation in a type 2 diabetes rat model. *Pharmacol Res*, 93:43-51. https://doi.org/10.1016/j.phrs.2015.01.001

Looker AC, Eberhardt MS, Saydah SH, 2016. Diabetes and fracture risk in older U.S. adults. *Bone*, 82:9-15. https://doi.org/10.1016/j.bone.2014.12.008

Lu JM, Wang YF, Yan HL, et al., 2016. Antidiabetic effect of total saponins from *Polygonatum kingianum* in streptozotocin-induced daibetic rats. *J Ethnopharmacol*, 179:291-300. https://doi.org/10.1016/j.jep.2015.12.057

Ma R, Wang L, Zhao B, et al., 2017. Diabetes perturbs bone microarchitecture and bone strength through regulation of Sema3A/IGF-1/β-catenin in rats. *Cell Physiol Biochem*, 41(1):55-66. https://doi.org/10.1159/000455936

Napoli N, Chandran M, Pierroz DD, et al., 2017. Mechanisms of diabetes mellitus-induced bone fragility. *Nat Rev Endocrinol*, 13(4):208-219. https://doi.org/10.1038/nrendo.2016.153

NCD Risk Factor Collaboration, 2016. Worldwide trends in diabetes since 1980: a pooled analysis of 751 population-based studies with 4.4 million participants. *Lancet*, 387(10027):1513-1530. https://doi.org/10.1016/S0140-6736(16)00618-8

Palsgaard J, Emanuelli B, Winnay JN, et al., 2012. Cross-talk between insulin and Wnt signaling in preadipocytes: role of Wnt co-receptor low density lipoprotein receptor-related protein-5 (LRP5). *J Biol Chem*, 287(15):12016-12026. https://doi.org/10.1074/jbc.M111.337048

Pelosi P, Lapi E, Cavalli L, et al., 2017. Bone status in a patient with insulin-like growth factor-1 receptor deletion syndrome: bone quality and structure evaluation using dual-energy X-ray absorptiometry, peripheral quantitative computed tomography, and quantitative ultrasonography. *Front Endocrinol (Lausanne)*, 8:227. https://doi.org/10.3389/fendo.2017.00227

Reed MJ, Meszaros K, Entes LJ, et al., 2000. A new rat model of type 2 diabetes: the fat-fed, streptozotocin-treated rat. *Metabolism*, 49(11):1390-1394. https://doi.org/10.1053/meta.2000.17721

Rota LM, Wood TL, 2015. Crosstalk of the insulin-like growth factor receptor with the Wnt signaling pathway in breast cancer. *Front Endocrinol (Lausanne)*, 6:92. https://doi.org/10.3389/fendo.2015.00092

Rota LM, Albanito L, Shin ME, et al., 2014. IGF1R inhibition in mammary epithelia promotes canonical Wnt signaling and Wnt1-driven tumors. *Cancer Res*, 74(19):5668-5679. https://doi.org/10.1158/0008-5472.CAN-14-0970

Schlupf J, Steinbeisser H, 2014. IGF antagonizes the Wnt/β-catenin pathway and promotes differentiation of extra-embryonic endoderm. *Differentiation*, 87(5):209-219. https://doi.org/10.1016/j.diff.2014.07.003

Schwartz AV, Hillier TA, Sellmeyer DE, et al., 2002. Older women with diabetes have a higher risk of falls: a prospective study. *Diabetes Care*, 25(10):1749-1754. https://doi.org/10.2337/diacare.25.10.1749

Siddle K, 2012. Molecular basis of signaling specificity of insulin and IGF receptors: neglected corners and recent advances. *Front Endocrinol (Lausanne)*, 3:34. https://doi.org/10.3389/fendo.2012.00034

Slaaby R, Schäffer L, Lautrup-Larsen I, et al., 2006. Hybrid receptors formed by insulin receptor (IR) and insulin-like growth factor I receptor (IGF-IR) have low insulin and high IGF-1 affinity irrespective of the IR splice variant. *J Biol Chem*, 281(36):25869-25874. https://doi.org/10.1074/jbc.M605189200

Solomon-Zemler R, Basel-Vanagaite L, Steier D, et al., 2017. A novel heterozygous IGF-1 receptor mutation associated with hypoglycemia. *Endocr Connect*, 6(6):395-403. https://doi.org/10.1530/EC-17-0038

Srinivasan K, Viswanad B, Asrat L, et al., 2005. Combination of high-fat diet-fed and low-dose streptozotocin-treated rat: a model for type 2 diabetes and pharmacological screening. *Pharmacol Res*, 52(4):313-320. https://doi.org/10.1016/j.phrs.2005.05.004

Sroga GE, Wu PC, Vashishth D, 2015. Insulin-like growth factor 1, glycation and bone fragility: implications for fracture resistance of bone. *PLoS ONE*, 10(1):e0117046. https://doi.org/10.1371/journal.pone.0117046

Szkudelski T, 2012. Streptozotocin-nicotinamide-induced diabetes in the rat. Characteristics of the experimental model. *Exp Biol Med (Maywood)*, 237(5):481-490. https://doi.org/10.1258/ebm.2012.011372

Thrailkill KM, Lumpkin CK Jr, Bunn RC, et al., 2005. Is insulin an anabolic agent in bone? Dissecting the diabetic

bone for clues. *Am J Physiol Endocrinol Metab*, 289(5): E735-E745. https://doi.org/10.1152/ajpendo.00159.2005

Yan Y, Du CH, Li ZY, et al., 2018. Comparing the antidiabetic effects and chemical profiles of raw and fermented Chinese Ge-Gen-Qin-Lian decoction by integrating untargeted metabolomics and targeted analysis. *Chin Med*, 13(1):54. https://doi.org/10.1186/s13020-018-0208-7

Zhang ZD, Ren H, Shen GY, et al., 2016. Animal models for glucocorticoid-induced postmenopausal osteoporosis: an updated review. *Biomed Pharmacother*, 84:438-446. https://doi.org/10.1016/j.biopha.2016.09.045

Zhao HH, Li ZG, Tian GH, et al., 2013. Effects of traditional Chinese medicine on rats with Type II diabetes induced by high-fat diet and streptozotocin: a urine metabonomic study. *Afr Health Sci*, 13(3):673-681. https://doi.org/10.4314/ahs.v13i3.22

中文概要

题　目：IGF-1R/β-catenin 信号通路在 2 型糖尿病性骨质疏松中的作用

目　的：探讨胰岛素样生长因子-1 受体（IGF-1R）/β-联蛋白（β-catenin）信号通路是否在糖尿病性骨质疏松（DOP）病理机制中起作用。

创新点：发现 IGF-1R/β-catenin 信号通路在 DOP 病理机制中起作用，可能是 DOP 潜在的治疗靶点。

方　法：收集 DOP 患者血清，使用酶联免疫吸附测定（ELISA）法检测 IGF-1R 水平。DOP 大鼠在 4 周高脂饲料喂养后给予链脲佐菌素建模，对照组大鼠在普通饲料喂养 4 周后再给予链脲佐菌素溶媒（柠檬酸钠缓冲液）。应用双能 X 线吸收法、生物力学测试和苏木精-伊红（HE）染色法分别评估椎体骨量、骨强度和骨组织形态。使用实时定量聚合酶链反应（qRT-PCR）和蛋白印迹法（western blotting）测定 IGF-1R、糖原合成酶激酶-3β（GSK-3β）和 β-catenin 表达及其蛋白磷酸化水平。

结　论：DOP 患者血清 IGF-1R 较对照组高。DOP 大鼠骨量、压缩强度明显减小，HE 染色显示 DOP 椎体骨组织形态明显受损，IGF-1R 信使 RNA（mRNA）表达上调，IGF-1R、GSK-3β 和 β-catenin 蛋白磷酸化增加。由此可见，IGF-1R/β-catenin 信号通路在 DOP 的病理机制中起作用，该发现将有利于后期 DOP 治疗靶点的开发。

关键词：糖尿病性骨质疏松；胰岛素样生长因子-1 受体；信号通路；发病机制